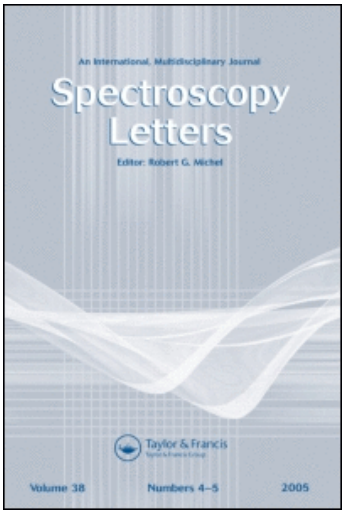

Spectroscopy Letters
Publication details, including instructions for authors and subscription information:
http://www.informaworld.com/smpp/title~content=t713597299

Spatial and Temporal Characterization of Distilled Water Plasma Using Laser-Induced Breakdown Spectroscopy: Effect of Self-Absorption on Plasma Parameters

S. Boussaïdi[a]; R. Hannachi[a]; H. Ghalila[a]; Z. BenLakhdar[a]; G. Taieb[b]
[a] LSAMA, Physics Department, Faculty of Sciences, University Tunis El Manar, Tunis, Tunisia [b] LPPM, Paris SUD University, Orsay, France

To cite this Article Boussaïdi, S. , Hannachi, R. , Ghalila, H. , BenLakhdar, Z. and Taieb, G.(2008) 'Spatial and Temporal Characterization of Distilled Water Plasma Using Laser-Induced Breakdown Spectroscopy: Effect of Self-Absorption on Plasma Parameters', Spectroscopy Letters, 41: 8, 369 — 375
To link to this Article: DOI: 10.1080/00387010802371973
URL: http://dx.doi.org/10.1080/00387010802371973

Spectroscopy Letters, 41:369–375, 2008

ISSN: 0038-7010 print/1532-2289 online
DOI: 10.1080/00387010802371973

Taylor & Francis
Taylor & Francis Group

Spatial and Temporal Characterization of Distilled Water Plasma Using Laser-Induced Breakdown Spectroscopy: Effect of Self-Absorption on Plasma Parameters

S. Boussaïdi[1], R. Hannachi[1], H. Ghalila[1], Z. BenLakhdar[1], and G. Taieb[2]

[1]LSAMA, Physics Department, Faculty of Sciences, University Tunis El Manar, Tunis, Tunisia
[2]LPPM, Paris SUD University, Orsay, France

ABSTRACT The spatiotemporal evolution of the plasma induced by interaction of an Nd-YAG laser pulse with the surface of distilled water is described. The temporal evolution from 200 ns after the plasma creation to 2200 ns of the H_α and H_β lines is reported. Supposing the local thermodynamic equilibrium, the two plasma parameters, electron density and temperature, are determined, including the influence of the self-absorption on its measurements. The spatial evolution of the H_β intensity and of the electron density is given.

KEYWORDS laser-induced plasma spectroscopy, plasma, self-absorption, spatial, temporal, water

INTRODUCTION

The technique of laser-induced breakdown spectroscopy (LIBS), where focusing the pulse of a laser on a surface forms luminous microplasma, is a powerful technique due to its rapidity and its case of use.[1] This technique has been developed over the past years for many applications,[2,3] including analytical chemistry, medical surgery, and material cleaning. For solid targets, analysis of the spectra emitted by the vaporized species (ions and neutral atoms essentially) gives information on their chemical compositions.[4,5] Less attention has been paid to the analysis of liquid by LIBS, as a number of alternative and classic analytical techniques have much higher sensitivity.

Cremers et al.[6] carried at the most advanced spectroscopic study on plasma created by laser into water. The object of their study was to detect the trace present into water using emission spectroscopy. The plasma is obtained by focusing an Nd:YAG into the sample. The pulse duration is about 15 ns. They obtained the temporal evolution of electronic temperature and density by means of the Li and Ca elements. The corresponding temperatures are between 6900 K and 11,600 K. The lines used for the determination of electron density are the doublet Li I (670.78 nm and 670.79 nm) and the Ca I line (422.7 nm). The precision of N_e is estimated to ±25%.

Received 17 April 2007; accepted 30 April 2008.

Address correspondence to S. Boussaïdi, LSAMA, Physics Department, Faculty of Sciences, University Tunis El Manar, Tunis, Tunisia. E-mail: boussaidi_slah@hotmail.fr

These lines are resonance lines; no verification or correction of the self-absorption effect was done. This may be critical, particularly for the Li I doublet, which is sensitive to this effect. Thus, it is possible that the electron densities may have been overestimated during the experiments of Cremers et al. Other point of fundamental importance is that all the spectra were integrated in the space, and no radial measurements of T_e or N_e were done.

We have determined both plasma electron density and temperature from analysis of the time-resolved spectra of the two hydrogen lines H_α and H_β, taking into account the auto-absorption phenomenon observed in the case of the H_α line. The spatial evolution of the electron density N_e was also determined by using the correlation between it and the Stark width of the atomic lines.

MATERIALS AND METHODS

In Fig. 1, we present the experimental setup. The second harmonic of an Nd-YAG laser (Quantel, France; model Brillant B) pulse at 532 nm, 10 ns duration, 30 mJ energy, at a repetition rate of 5 Hz, is focused on the surface of the sample (distilled water) by a lens of 15 cm focal length (L2). The plasma emission is collected by another lens of 10 cm focal length (L1) on the entrance slit of a 60-cm focal length monochromator (Gzerny–Turner, USA). The distance between the plasma P and the slit is 60 cm. The lens L1 is set a distance $d_1 = 12.6$ cm from P in order to obtain an image magnification of ≈ 4, making easier the study of the spatial evolution of P. The signal is collected by an ICCD camera (Andor, Belfast, Northern Ireland; model *istar*) in which the matrix CCD is composed of a 1024×512 photocathode connected to a PC for signal analysis under software control, and it caters to a broad range of spectroscopic applications. The spectra were acquired using a gate time of 200 ns, which provided a good signal-to-noise ratio, necessary for a precise measurement of the spectral line intensities. The time delays after the laser pulse ranged between 200 ns and 2200 ns.

Plasma Parameters

A lot of studies have been performed to investigate the shape of the hydrogen line behavior and eventually its broadening.[7] We present here briefly the different theoretical approaches used. The electron impact theory considers the broadening as a result of the impacts of the free electrons in the plasma (impact approximation). As a consequence, the amount of the broadening depends on the electron concentration and on a logarithmic factor that decreases with an increase of the electron density. In the quasi-static approximation, the broadening depends on the electron density for singly ionized ions to the power of two thirds. This power law still holds true after accounting for ion–ion correlation and Debye shielding effects. Assuming that the collisions by electrons are predominant in the plasma

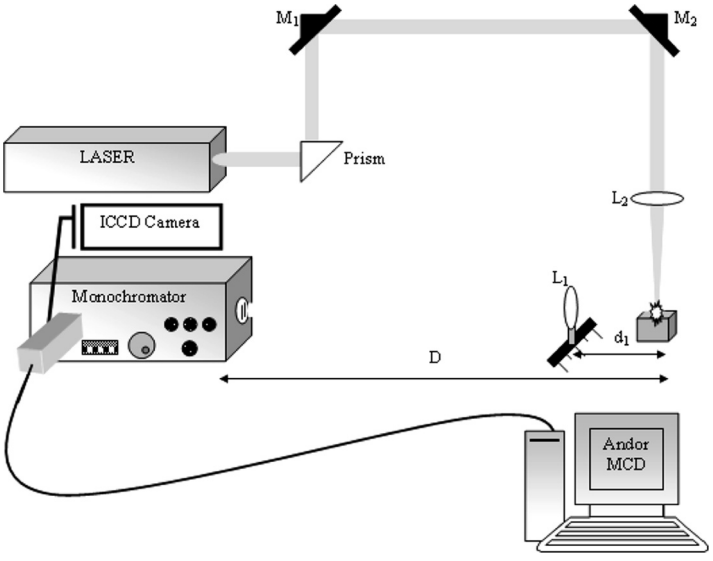

FIGURE 1 Experimental setup.

produced by the Nd-YAG laser used and that this plasma is at local thermodynamic equilibrium (LTE). The determination of the electronic density and temperature is fundamental. In fact, the electronic temperature describes the population of the excited states using the Boltzmann law.[8,9] On the other hand, the electronic density is frequently used to study the thermodynamic properties of the plasma and also the collisional process. In the current work, we will try to determine these parameters and their evolution in time. The determination of the electronic temperature and density will serve us to judge whether the plasma is under LTE conditions or not. In this study, plasma inhomogeneity was neglected because the gradient was not very strong. In general, however, the gradient of temperature and density is strong except for the first few millimeters from the target surface. Thus, the spatial evolution that we will present later confirms this supposition. In Fig. 2 we present the temporal evolution of H_α at 656.28 nm (Fig. 2a) and H_β at 486.13 nm (Fig. 2b),[10] in the time interval 200–2200 ns. These lines are useful to determinate the electron plasma temperature (T_e) obtained from the measurement of the ratio of their intensities[11] as follows:

$$\frac{I_1}{I_2} = \left(\frac{g_1 A_1}{\lambda_1}\right)\left(\frac{\lambda_2}{g_2 A_2}\right) \times \exp\left[\frac{-|E_1 - E_2|}{kT_e}\right]. \quad (1)$$

The precision on the intensities is estimated at 3% using the reproducibility on the line emission intensity, so we obtain incertitude on the temperature of about 5%. Here I, λ, A, and g are respectively the total emission intensity (integrated over the profile), the wavelength, the transition probability, and the statistical weight of the two lines, respectively, and E_1 and E_2 are the energies of the emitting levels. The first estimation of the temporal evolution of the electron temperature shows an exponential decay ($\tau \approx 455$ ns), at in can be seen in Fig. 3.

The emission profiles of the hydrogen Balmer lines can be affected by different kinds of broadening, including natural, Doppler, Stark, instrumental (in our case the instrumental broadening is about 0.03 Å), and so forth.[11] The Stark effect is linear for hydrogen and hydrogenic lines.[1] Due to this effect, hydrogen lines are broadened and therefore more sensitive to the plasma electron-number density,[12] and the width of Stark-broadened spectral lines in plasma depends on the electron density N_e.[1] A lot of studies has been carried out to calculate the electron densities; it was shown that for an accurate determination of the electron density in the range of 10^{15} to $3 \times 10^{17}\,\mathrm{cm}^{-3}$, the H_β line is frequently

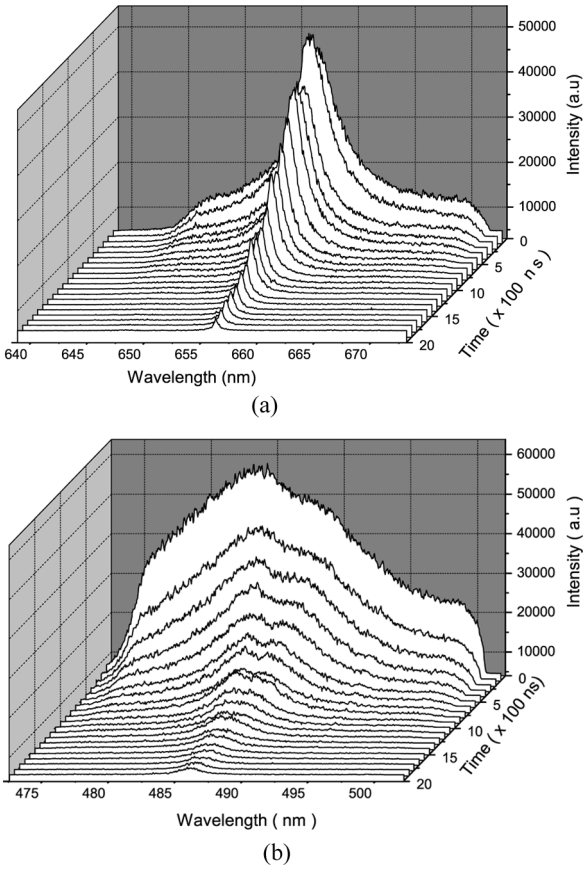

FIGURE 2 **(a) Temporal evolution of the H_α-line at 656.28 nm. (b) Temporal evolution of the H_β-line at 486.13 nm.**

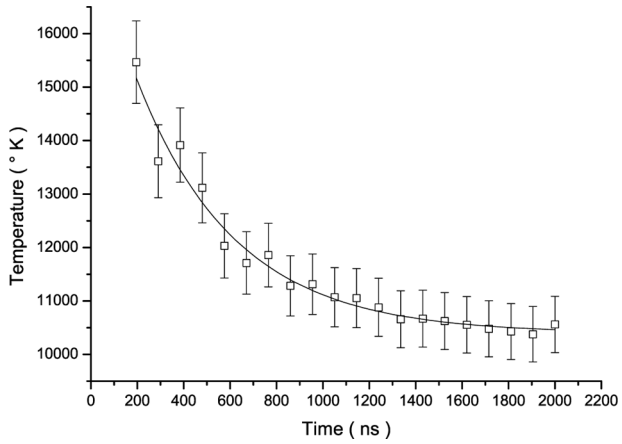

FIGURE 3 **First estimation of the temporal evolution of electron temperature fitted with an exponential decay.**

used.[13,14] The comparison of the theoretical and experimental results of widths using the H_β line presents reliability better than 5%.[7] In the current work, we enlarge this range and we estimate that the calculation of the H_β-line width is still available untill $4.5 \times 10^{17}\,cm^{-3}$ and it confirms the fact that at electron densities higher than $5 \times 10^{17}\,cm^{-3}$, the H_β-line width is affected by other phenomena[15] such as strong broadening, which introduces the asymmetry between the red and the blue peaks, and distortion of the line, which may be caused by the self-absorption effect.[16] Many theoretical and numerical studies were performed to determinate the electron density. The most frequently used tables for this purpose were evaluated by Vidal, Cooper, and Smith using the unified theory.[17] One of these methods is presented by Joviçeviç et al.,[12] and Helbig,[18] who calculated the Stark width including the Doppler and instrumental broadening, gives the following relation between the Stark half-width at half-maximum (HWHM) of the H_β line and the electron density N_e.

$$N_e(\mathrm{cm}^{-3}) = 10^{16} \times (\mathrm{HWHM}/4.7333)^{1.49}. \quad (2)$$

Because the gradient of temperature is present and for a convenient spatial diagnostic of the plasma, the formula (2) will be useful later to evaluate the spatial evolution of the electron density. The method used for the temporal evolution of the electron density is given by Griem;[7] this is a theoretical approach based on semiclassical theory and it shows its performance for dense plasma. The stark full-width at half-maximum (FWHM) is related to the electron density by[7]

$$N_e(\mathrm{cm}^{-3}) = C(N_e, T_e) \times \mathrm{FWHM}^{3/2}, \quad (3)$$

where C is a parameter that is tabulated for the H Balmer lines in the literature[7] and which depends weakly on N_e and T_e. We represent in Fig. 4 the temporal evolution of the electron density calculated from the H_α and H_β line Stark widths.

Knowing the values of electronic temperature and density, we can affirm the existence of LTE in the range of time mentioned before. Using the criterion given by Griem on the electron density:[7]

$$N_{e0} = 1.6 \times 10^{12} \times (\Delta E)^3 \times T_e^{1/2},$$

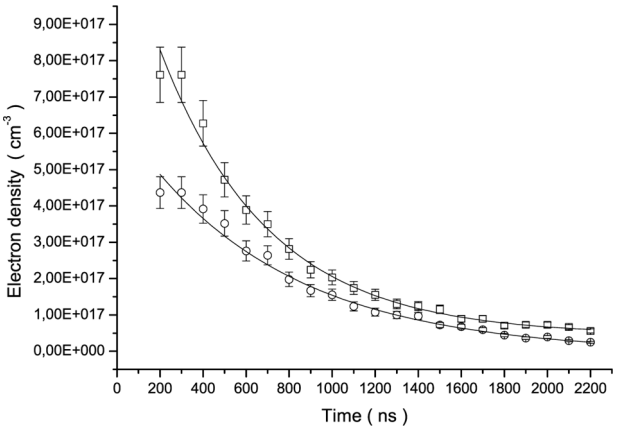

FIGURE 4 **Temporal evolution of electron density calculated from (□) H_α line width and (○): H_β line width.**

where ΔE is the difference between the two upper levels of the considering species, and T_e is the electronic temperature obtained previously. We obtain the value of $N_{e0} \approx 4 \times 10^{14}\,cm^{-3}$, and thus verify that our plasma is under LTE as our density values are greater than N_{e0}.

Effect of Self-Absorption on the Plasma Parameters Determination

Due to the presence of a relatively cold layer at the periphery of the expanding plasma, the lines emitted from the target species can be strongly self-absorbed and become optically thick.[7] Therefore, the measurements of electron density and temperature using these lines are likely to be affected by strong errors. It is shown that for high densities, the H_α line is self-absorbed, thus making the electron density overestimated.[16] Indeed the self-absorption increases the width at half-maximum of the line and decreases its intensity.[19] And the measurement of the broadening of the line used for the determination of T_e and N_e has to be corrected.

We propose here a simple method that can be used for quantifying the effect of self-absorption on the emission lines profiles observed by LIBS. We suppose first that the plasma is homogenous and we neglect the gradient of temperature and density. The self-absorption coefficient is defined as the ratio of the measured peak height to peak height of the line non–self-absorbed. This coefficient is equal to one if the line is optically thin and decrease to zero if it becomes thick.[20]

The ratio of the intensities is given by

$$\frac{I_0^{thin}}{I_0^{thick}} = \frac{\tau_0}{(1-\exp(-\tau_0))}, \quad (4)$$

where τ_0 is the optical thickness.

In the other side, the ratio of the (FWHM), which is also affected by the self-absorption, is given by the formula

$$\frac{\Delta\omega^{thin}}{\Delta\omega^{thick}} = \frac{\Delta\lambda^{thick}}{\Delta\lambda^{thin}} = \left(-1 - \frac{\tau_0}{Ln\left(\frac{1+\exp(-\tau_0)}{2}\right)}\right)^{-1/2}. \quad (5)$$

We'll introduce in this work the so-called correction factor (CF) defined by

$$\mathrm{CF} = I_0^{thin} \times \Delta\lambda^{thick}/I_0^{thick} \times \Delta\lambda^{thin}. \quad (6)$$

We present in Fig. 5 the variation of these values versus the optical thickness (4, 5, and 6).

The variation of the correction factor plotted with the ratio $\Delta\lambda^{thick}/\Delta\lambda^{thin}$ is shown in Fig. 6. The plot is fitted by a simple function given by

$$\mathrm{CF} = (\Delta\lambda^{thick}/\Delta\lambda^{thin})^{0.773}. \quad (7)$$

As mentioned previously, the electron density calculated from the H_β line is better than the one calculated from the H_α line, but we shouldn't forget the fact that this one is self-absorbed. Hence we presume that the electron density calculated from the H_β line

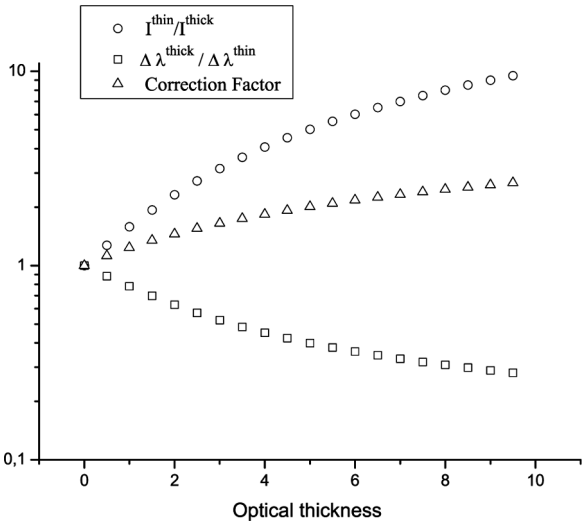

FIGURE 5 Evolution of (○)I^{thin}/I^{thick}; (□) $\Delta\lambda^{thick}/\Delta\lambda^{thin}$ and (Δ) C.F versus a random optical thickness.

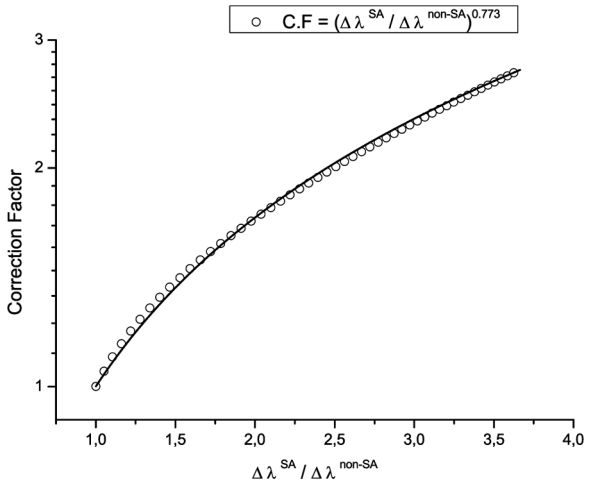

FIGURE 6 $\mathrm{CF} = (\Delta\lambda^{thick}/\Delta\lambda^{thin})^{0.773}$.

is the real value. We have deduced from the values of densities (using the H_β line) given in equation (3) the values of the Stark FWHM that the H_α line should have if it was non self-absorbed, and then calculated the value of $\Delta\lambda^{SA}/\Delta\lambda^{non\text{-}SA}$, and we calculate the correction factor using the expression (7). The variation of the CF with the ratio of the integral intensities is given by the expression calculated by M.El Sherbini et al.[20]:

$$\mathrm{CF} = (\tilde{I}^{thin}/\tilde{I}^{thick})^{0.5}. \quad (8)$$

Finally, to get the corrected temperature values that are reported in the graph presented in Fig. 7, one uses the equations (7) and (8) and then corrects the intensity of the H_α line. The temperature calculated after the self-absorption correction is less than the temperature calculated and presented in Fig. 3. In fact, the self-absorbed lines are generally followed by a decrease of peak intensity; for this reason, the temperature calculated before is higher than the one calculated after including a correction due to the self-absorption. The temporal evolution of the electronic temperature presents an exponential decay as can be observed in the two cases, nevertheless this decay is smoother in the first case (≈455 ns) than in the second one (≈402 ns). The current method can be generalized for any plasma induced by laser ablation. In fact, this method can optimize with a high precision the electronic temperature values that are highly used for a quantitative study of the plasma. Nevertheless, one must use lines whose Stark parameters are known with good precision.

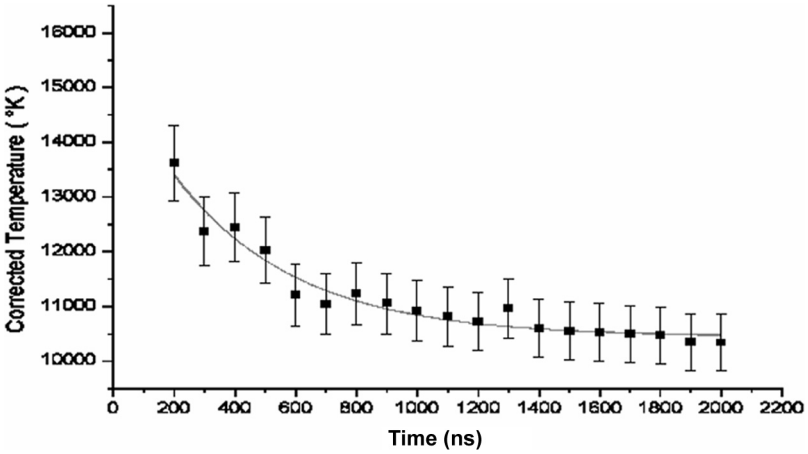

FIGURE 7 **Temporal evolution of T_e corrected.**

Spatial Evolution of the H_β Line

We have recorded the spatial emission of the H_β line by moving horizontally the collecting lens L1 by a step of 0.5 mm on a total horizontal width of 3 mm. These results, recorded at the time intervals 0.5 μs, 1 μs, and 2 μs after the laser pulse, are shown in Fig. 8. In order to investigate the behavior of the plasma, we have chosen to study among different parameters the spatial evolution of the electron density. The electron density can be calculated by using the HWHM of the H_β line already studied, applied in equation (2). These results are presented in Fig. 8. As can be seen from the figure, the radial gradient of the electron density is much smaller than the radial gradient of the intensity, which depends strongly on r, and it decreases quickly. Because the electronic density depends on the Stark width and there are no significant differences of the Stark widths[21] on both sides of the center of the plasma, therefore the electron density should not differ very much in radial direction. These results do not contradict the results found by other authors.[21,22] The density profile is practically flat, this behavior confirms the spatial plasma homogenity, nevertheless the profile is smoother at 0.5 μs and at 1 μs more than at 2 μs,

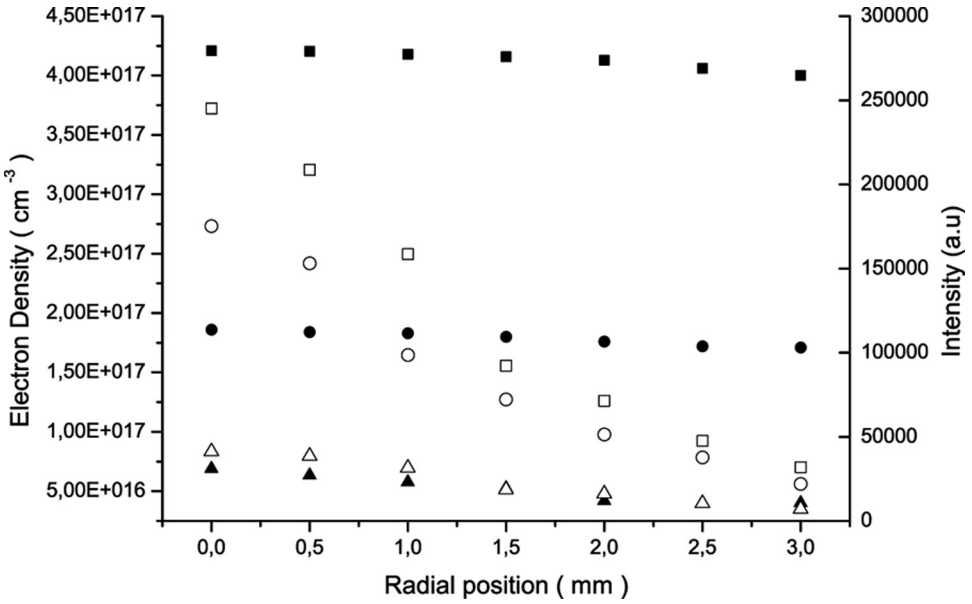

FIGURE 8 **■, ●, and ▲: Spatial evolution of the electron density. □, ○, and △: Spatial evolution of the intensity. ■, □: $t = 0.5$ μs; ●, ○: $t = 1$ μs. ▲, △: $t = 2$ μs.**

and we can attribute this to the plasma expansion. The plasma expansion explains also the intensity profile. However, the interaction with the ambient air has also a strong influence on the expansion process.[23] The drop of density to zero characterizing the plasma–air boundary is not observed, which supposes that the plasma geometry could not be cylindrical, therefore a hemispheric geometry[24] could explain this behavior but not in our experimental conditions where, and especially at the edges of the plasma, the geometry is not regular.

CONCLUSIONS

We have presented in this present work the results of the measurements of two parameters (electronic density and temperature) used to describe the plasma formed by interaction of laser pulses on the surface of pure water, including corrections due to the self-absorption of the H_α line. The correction factor introduced in these corrections allows as to obtain a correct estimation of the plasma temperature during its formation and its evolution. However, one must know a Stark width (i.e., electron density) of at least one line with good precision in order to evaluate the correction factor, which will serve to correct the electron temperature. Results on the spatial distribution of intensities and electron density are given. The spatial evolution of the integrated intensities could be used to determine the emissivity of the plasma by applying the Abel inversion,[7] as the intensities measurements reported here are averaged over the radial distribution. Hence, this study would be useful to describe plasmas induced by laser ablation especially on liquid surfaces.

REFERENCES

1. Samek, O.; Beddows, D. C. S.; Kaiser, J.; Kukhlevsky, S. V.; Liska, M.; Telle, H. H.; Young, J. Application of laser-induced breakdown spectroscopy in situ analysis of liquid samples. *Opt. Eng.* **2000**, *39* (8), 2248–2262.
2. De Giacomo, A.; Shakhatov, V. A.; Senesi, G. S.; Orlando, S. Spectroscopic investigation of the technique of plasma assisted pulsed laser deposition of titanium dioxide. *Spectrochim. Acta B Atom. spectrosc.* **2001**, *56*, 1459–1472.
3. Rusak, D. A.; Castle, B. C.; Smith, B. W.; Winefordner, J. D. Fundamentals and applications of laser-induced breakdown spectroscopy. *Crit. Rev. Anal. Chem.* **1997**, *27*, 257–290.
4. Smith, W. L.; Liu, P.; Bloembergen, N. Superbroadening in H_2O and D_2O by self-focused picosecond pulses from a YAlG: Nd laser. *Phys. Rev. A* **1997**, *15*, 2396.
5. Wallis, F. J.; Chadwick, B. L.; Morrison, R. J. S. Analysis of lignite using laser-induced breakdown spectroscopy. *App. Spectrosc.* **2000**, *54*, 8.
6. Cremers, D. A.; Radziemski, L. J.; Loree, T. R. Spectrochemeical analysis of liquids using laser spark. *App. Spectrosc.* **1984**, *38*, 721–729.
7. Griem, H. R. *Plasma Spectroscopy*; McGraw-Hill: New York, 1964.
8. Milan, M.; Laserna, J. J. Diagnostics of silicon plasmas produced by visible nanosecond laser ablation. *Spectrochim. Acta B* **2001**, *56*(3), 275–288.
9. Vaquié, S. *L'arc électrique*. CNRS Edit: France, 2000.
10. Striganov, S. *Tables of Spectral Lines of Neutral and Ionized Atoms*; IFI/Plenum: New York, 1968.
11. Qayyum, A.; Ahmad, R.; Ghauri, S. A.; Waheed, A.; Zakaullah, M. Hydrogen Balmer-β and Balmer-γ emission profiles in an abnormal glow region of hydrogen plasma. *Vacuum* **2006**, *80*, 574–580.
12. Joviçeviç, S.; Ivkoviç, M.; Pavloviç, Z.; Konjeviç, N. Parametric study of an atmospheric pressure microwave-induced plasma of the mini MIP torch—I. Two-dimensional spatially resolved electron-number density measurements. *Spectrochim. Acta B* **2000**, *55*, 1879–1893.
13. Lochte-Holtgreven, W. Plasma *Diagnostics*; North Holland: Amsterdam, 1968; 135–210.
14. Escarguel, A.; Ferha, B.; Lesage, A.; Richou, J. A single laser spark in aqueous medium. *J. Quant. Spectrosc. Radiat. Transfer* **2000**, *64*, 353–361.
15. El Sherbini, A. M.; El Sherbini, Th.M.; Hegazy, H. Measurement of electron density utilizing the H_α-line from laser produced plasma in air. *Spectrochimi. Acta B* **2006**, *61*, 532–539.
16. Ashkenazy, J.; Kipper, R.; Caner, M. Spectroscopic measurements of electron density of capillary plasma based on Stark broadening of hydrogen lines. *Phys. Rev. A* **1991**, *43*(10), 5568–5574.
17. Vidal, C. R.; Cooper, J.; Smith, E. W. Hydrogen Stark-broadening tables. *Astrophys. J.* **1973**, *25*(suppl. 214), 37–36.
18. Helbig, V.; Nick, K. P. Investigation of the Stark broadening of Balmer beta. *J. Phys. B At. Mol. Phys.* **1981**, *14*, 3573–3583.
19. Amamou, H.; Bois, A.; Ferhat, B.; Redon, R.; Rossetto, B.; Matheron, P. Correction of self-absorption spectral line and ratios of transition probabilities for homogeneous and LTE plasma. *J. Quanti. Spectrosc. Radiat. Transfer* **2002**, *75*, 747.
20. El Sherbini, A. M.; El Sherbini, Th.M.; Hegazy, H.; Cristoferetti, G.; Legnaioli, S.; Palleschi, V.; Parddini, L.; Salvetti, A.; Tognoni, E. Evaluation of self-absorption coefficients of aluminum emission lines in laser-induced breakdown spectroscopy measurements. *Spectrochim. Acta B* **2005**, *60*, 1573–1579.
21. Zhao, X. Z.; Shen, L. J.; Lu, T. X.; Niemax, K. Spatial distributions of electron density in microplasmas produced by laser ablation of solids. *Appl. Phys. B* **1992**, *55*, 327–330.
22. Barthélemy, O.; Margot, J.; Chaker, M.; Sabsabi, M.; Vidal, F.; Johnston, T. W.; Laville, S.; Le Drogoff, B. Influence of the laser parameters on the space and time characteristics of an aluminum laser-induced plasma. *Spectrochim. Acta B* **2005**, *60*, 905–914.
23. Garrelie, F.; Champeaux, C.; Catherinot, A. Expansion dynamics of the plasma plume created by laser ablation in a background gas. *Appl. Phys. A* **1999**, *69*, S55–S58.
24. Barthélemy, O.; Margot, J.; Chaker, M. Characterization of the expansion of an aluminum laser-induced plasma in ambient air by fast photography. *IEEE Trans. Plasma Sci.* **2005**, *33*, 476–477.